Analysis of catalytic oxidation of aromatic hydrocarbons over supported palladium catalyst with different pretreatments based on heterogeneous adsorption properties

Wang Geun Shim [a], Jae Wook Lee [b], Sang Chai Kim [c],*

[a] School of Applied Chemical Engineering, Chonnam National University, 300 Yongbong-dong, Buk-gu, Gwangju 500-757, Republic of Korea
[b] Department of Chemical and Biochemical Engineering, Chosun University, 375 Seosuk-dong, Dong-gu, Gwangju 501-759, Republic of Korea
[c] Department of Environmental Education, Mokpo National University 61 Dorim-ri, Cheonggye-myeon, Muan-gun, Jeonnam 534-729, Republic of Korea

ABSTRACT

We investigated the catalytic oxidation and adsorption of benzene, toluene, and o-xylene (BTX) by using the palladium (Pd)-based catalyst and its pretreated (pre-oxidized and pre-reduced) catalysts. The physico-chemical properties of the catalysts were characterized and confirmed by using several reliable methods such as the Brunauer Emmett Teller (BET) surface area analysis, gravimetric adsorption analysis, light-off curves analysis, and X-ray photoelectron spectroscopy (XPS). The adsorption and catalytic activities of the catalysts were found to be closely connected with the pretreatment methods and temperatures. Especially, the hydrogen treated catalysts with a largely metallic form enhanced the adsorption ability and catalytic activity of toluene compared to that of the parent and air treated catalysts. In addition, the adsorption equilibrium isotherms of BTX on pre-reduced catalyst at three different temperatures were analyzed successfully with the two sites localized Langmuir (L2m) isotherm equation. Moreover, the strong correlations between the catalytic behavior and the adsorption properties of BTX were explained in terms of adsorption affinity, isosteric heat of adsorption, and adsorption energy distributions.

© 2008 Elsevier B.V. All rights reserved.

1. Introduction

Developing reliable methods of controlling the emission of volatile organic compounds (VOCs) is of great importance because of their harmful effects on human health and the environment. In general, the catalytic oxidation of VOCs has been considered as one of the well-established technologies available such as oxidation, adsorption, absorption, etc. Compared to the common thermal oxidation, the distinguished characteristics of catalytic oxidation are (1) low thermal NO_x emissions, (2) high destructive efficiency, (3) low energy cost and (4) a relatively high flexibility [1–4].

On the other hand, the proper selection and development of the catalyst is essential for successful removal of VOCs. Currently, various kinds of catalysts such as supported noble metals, metal oxides, and mixtures of noble metals and metal oxides are being extensively used for the complete oxidation of VOCs with different advantages and limitations. Considering the activity, selectivity and stability of the catalysts for catalytic oxidation, supported noble metals have been generally regarded as the most desirable

catalysts despite their low resistance to deactivation and high cost for pure component. In addition, previous studies have shown that the main advantages of palladium (Pd)-based catalysts are high activity, thermal stability, performance and low cost compared to the platinum (Pt)-based catalysts, although they have a relatively higher susceptibility to sulfur containing pollutants [5–11].

Recently, many researchers have reported that the performance of Pd supported catalysts for the oxidation of VOCs is highly dependent on the oxidation state of Pd. In other words, pre-reduced Pd catalysts largely having metallic species (Pd^0) are more active than the pre-oxidized Pd catalysts existing mainly in the oxide form (PdO/Pd^{2+}) [5,9,10,12–16]. Until now, considerable research effort has been mostly concentrated on the understanding of the role of the active Pd phase on the catalytic activity. However, little attention has been given to the investigation of the influence of the surface state on adsorption properties and the relationship between the adsorption and the catalytic activities of VOCs [16–19]. It has been known that the catalytic activities of catalysts for aromatic molecules are closely connected with the interrelation of the reactant and the catalyst. The main factors in controlling the activity sequence are the strength of adsorption (adsorption affinity and heat of adsorption), the order of ionization potentials (or Debye dipole moment), and the strength of the weakest C–H

bond in the molecule [15,20–25]. It seems, therefore, that a systematic approach to adsorption and catalytic oxidation of the Pd-based catalyst may provide some information on the role of the oxidation state of supported Pd with respect to adsorption equilibrium and catalytic oxidation of VOCs. Thus, in this work, we investigated the influence of pretreatments (air and hydrogen) on the adsorption and catalytic activities of different aromatic hydrocarbons over the Pd-based catalyst. Especially, benzene, toluene and o-xylene (BTX) were chosen as model compounds for their toxic, carcinogenic and different molecular properties. Finally, we present our interpretation of thermodynamic parameters such as isosteric heat of adsorption, adsorption affinity and adsorption energy distribution as well as its light-off (or ignition) curves and X-ray photoelectron spectroscopy (XPS) analysis.

2. Experimental

2.1. Catalyst preparation and characterization techniques

The catalyst was prepared by using a conventional incipient wetness impregnation method with an aqueous solution of $Pd(NO_3)_2$ (Johnson Matthey). δ-Al_2O_3 (Showa Aluminum) was used as support for Pd-based catalyst. The catalyst contained 0.3 wt% Pd and was denoted as Pd-0.30. The impregnated supports were dried at 120 °C overnight and calcined at 400 °C for 4 h in a crucible. The prepared catalysts were pelletized, crushed and then finally sieved to obtain the particles with a diameter of 0.2–0.3 mm for the adsorption and catalytic activity measurements. The net amount of Pd over the parent catalyst was measured by Inductively Coupled Plasma (ICP) using a PerkinElmer OPTIMA 4300DV. Pretreatment was also performed at three different temperatures of (200, 300 and 400) °C for 2 h with hydrogen (100 cm^3 min^{-1}) and air (100 cm^3 min^{-1}) to investigate the influence of gas treatments on the catalytic activities and adsorption characteristics of VOCs. The specific surface areas (S_{BET}) of the catalysts were measured by nitrogen adsorption at liquid nitrogen temperature (-196 °C) using a Micromeritics ASAP 2020 analyzer. An X-ray photoelectron spectroscopy analysis was conducted using a photoelectron spectrometer VG Scientific MultiLab 2000 system equipped with a non-monochromatic Mg Kα radiation of 1253.6 eV. The C1s peak (285.0 eV) was used to calibrate the binding energy (BE) values.

Hydrogen chemisorption measurements (ChemBET 3000) were performed using the excess pulse technique to measure the metal surface area. Catalyst samples of 0.4 g were first purged by a nitrogen flow (90 cm^3 min^{-1}) to remove moisture. Then, the catalysts were reduced by a hydrogen flow containing 5 vol.% H_2 (90 cm^3 min^{-1}) at 400 °C for 1 h, and finally cooled down to room
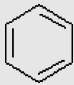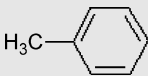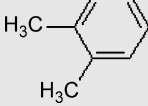
temperature in a stream of nitrogen. The metal surface area was measured by hydrogen chemisorption uptake at room temperature. A pulse of H_2 of known volume was injected into a N_2 carrier stream and the amount of H_2 chemisorbed by the sample was determined from the difference in TCD response before and after passage across the detector.

2.2. Catalytic oxidation and adsorption of BTX

The basic properties of BTX were summarized in Table 1. The purity and manufacturer of each BTX are as follows: benzene, 99.5% (Junsei Chemical Co.); toluene, 99.5% (Junsei Chemical Co.); o-xylene, 95.0% (Junsei Chemical Co.). All chemicals were used as received without further treatment. BTX complete oxidations were carried out using a conventional fixed bed flow reactor as reported in our previous work [25]. The reactor had three major sections namely (i) apparatus for preparation of vapors, (ii) fixed bed flow reactor in a heating system, and (iii) apparatus for the analysis of reactants and products. The catalytic reactor (quartz tube with the shape of a Y) consisted of a vertical tubular of 1.2 cm diameter and 35 cm length in an electrical heating system controlled by a proportional integral derivative (PID) controller. In each run, 1 g of catalyst was loaded in the middle of the reactor supported by quartz wool. For accurate and stable controlling of the gas flow rates, mass flow controllers (UNIT Instrument, UFC-8100) were used. The concentration of each component was 1000 ppm, which was controlled by the temperature of the saturator and the mass flow controller. The flow rate of the gas mixture through the reactor was 100 cm^3 min^{-1}, which gave a gas hourly space velocity (GHSV) of 8000 h^{-1}. All the lines were heated sufficiently at 120 °C to prevent the adsorption and condensation of the reactant and the product in the tubes. The concentration of inlet and exit gas stream was determined using a gas chromatograph GC-14A model (Shimadzu) equipped with thermal conductivity. The GC/MS (Shimadzu, QP5050) was also employed for the quantitative and qualitative analysis of the products and by-products. Apart from the products such as CO_2 and H_2O, no other by-products were found in most of the experiments. Thus, the conversion was calculated based on the hydrocarbon consumption.

The single component adsorption amount was measured by a quartz spring balance, which was placed in a closed glass system [26,27]. A given amount (0.1 g) of catalysts was charged in a small quartz basket, which was attached to the end of the quartz spring. Catalyst samples were weighed with an accuracy of ±0.01 mg. Prior to the equilibrium experiments, the catalysts were outgassed under vacuum condition for 12 h at 10^{-3} Pa and 250 °C for the complete removal of impurities. A turbomolecular pump (Edward type EXT70) in combination with a rotary vacuum pump (Edward

Table 1
The basic properties of benzene, toluene and o-xylene

Adsorbate	Structure	Molecular weight	Debye dipole moment	Ionization potential (eV)
Benzene		78	0.0	9.3
Toluene	H_3C—	92	0.4	8.8
o-Xylene	H_3C—, H_3C	106	0.5	8.5

model RV5) was used to evacuate the system. Pirani and Penning vacuum gauges (Edwards Series 1000) were used for the measurement of vacuum. The pressure of the system was measured using a Baratron absolute pressure transducer (MKS instruments type 128) with an accuracy of $\pm0.15\%$ and a power supply read-out instrument (Type PDR-C-1C). The variation of mass was measured by a digital voltmeter that was connected to the spring sensor. The adsorption experiments were carried out at three temperatures of (150, 175 and 200) °C, respectively.

3. Results and discussion

3.1. Catalytic oxidation and adsorption of toluene

To understand the influence of surface treatments on the adsorption and catalytic activities of BTX over the catalyst, two different gases of air and hydrogen were used. Table 2 compares the BET surface areas of Pd-0.30 and its air and hydrogen pretreated catalysts. As presented in Table 2, the negligible differences between the BET surface areas indicated the insignificant effect of the pretreatment temperatures and the pretreatment methods on the textural properties.

The light-off (or ignition) curves were used to compare the catalytic activity of the catalysts for VOCs oxidation. The conversion was calculated on the basis of hydrocarbon consumption as described in Section 2. Before conducting the complete oxidation of toluene over the parent and pretreated catalysts, a blank test was performed to check the existence of homogeneous reactions. The blank test detected no thermal (or homogeneous) oxidation of toluene at a temperature below 600 °C. This result indicates that the employed system may be applied for analyzing the catalytic oxidation of VOCs. Table 2 also presents the reaction temperatures of 10% (T_{10}), 50% (T_{50}) and 90% (T_{90}) for toluene conversion (1000 ppm in air) over the parent sample (Pd-0.30) and its air (or oxidized), and hydrogen (or reduced) catalysts. Fig. 1(a) also shows the comparison plot of the reaction temperatures for T_{10}, T_{50} and T_{90} over Pd-0.30, air treated Pd-0.30 (300 °C) and hydrogen treated Pd-0.30 (300 °C). These results clearly support that the hydrogen treatment is a useful methodology of improving the catalytic properties of the Pd-based catalyst. These experimental findings reveal that the pre-reduced catalysts are more active than the pre-oxidized and parent catalysts. The order of catalytic activity based on reaction temperatures (T_{10}, T_{50} and T_{90}) was the pre-reduced catalyst > the parent > the pre-oxidized catalyst. In addition, the pretreatment temperature was observed to play a key role on the activity of the hydrogen treated catalyst. For example, in the case of hydrogen treated samples, the order of activity observed was 300 °C > 200 °C > 400 °C. However, the oxidation of toluene over the air treated catalysts slightly decreased in the order of 400 °C > 200 °C ≥ 300 °C. No distinct

relationship was observed between the order of catalytic activity for toluene conversion and the BET surface areas.

On the other hand, it is interesting to note that the differences in the catalytic activity are closely related with the oxidation state of Pd and the adsorption property. The XPS analyses provided some useful information on the surface state of the catalyst. It is generally known that the binding energy value of Pd $3d_{5/2}$ at 336.6 eV represents the characteristic of PdO (Pd^{2+}) and the XPS peak of metallic state of palladium (Pd^0) is exhibited at 334.8 eV [12]. In this work, however, the BE values of the parent and the pre-oxidized catalyst approached the oxidized state of 335.94 eV for the parent and 336.49 eV for the air pretreated sample. In addition, as shown in Fig. 1(b), the XPS peaks of the catalyst reduced at three different temperatures of 200, 300 and 400 °C appeared at 334.96, 334.56 and 335.00 eV, respectively. These results indicate that the parent sample was greatly reduced after the pretreatment with hydrogen at three different temperatures, suggesting the existence of metallic palladium (Pd^0). Especially, the metallic state of the sample is highly dependent on the reduction temperature and is closely related with the catalytic activity of toluene oxidation. In other words, the sample pre-reduced at 300 °C has relatively stabilized form and it requires the lowest reaction temperature for the complete oxidation compared to that of other pretreated temperatures. This finding also reveals that the pre-reduced samples actually were reoxidized after the oxidation of toluene regardless of the pretreatment temperature. Fig. 1(c) shows adsorption equilibrium amount of toluene on Pd-0.30, air treated Pd-0.30 (300 °C) and hydrogen treated Pd-0.30 (300 °C) at 150 °C. As shown in this figure, the adsorption capacity is closely related with the oxidation state of the Pd, which is a clear indication that hydrogen treated catalyst containing a metallic species has the highest adsorption amount of toluene. However, the result has no relevance to the general order of the BET surface area of pretreated catalyst. These findings also support that the oxidation state of Pd has a strong influence on both the catalytic activity and adsorption capacity of the catalyst just as previous studies have shown that the adsorption properties of the catalyst are closely connected to the concentration of acid sites on the support and the interaction between the oxidation state of the catalyst and the support [16,28,29].

3.2. Catalytic oxidation and adsorption of other aromatics

3.2.1. Catalytic oxidation

On the basis of the results reported above, the hydrogen pretreated catalysts (Pd-HT (300 °C)) were chosen for further evaluation of the adsorption and the catalytic properties of other aromatic VOCs. It has been suggested that in the case of Pd-based catalyst, the catalytic activities for the complete oxidation of BTX are in the order of toluene > o-xylene > benzene, which is directly

Table 2
BET surface areas and comparison of conversion temperatures for toluene oxidation over parent (Pd-0.30) and its pretreated catalysts

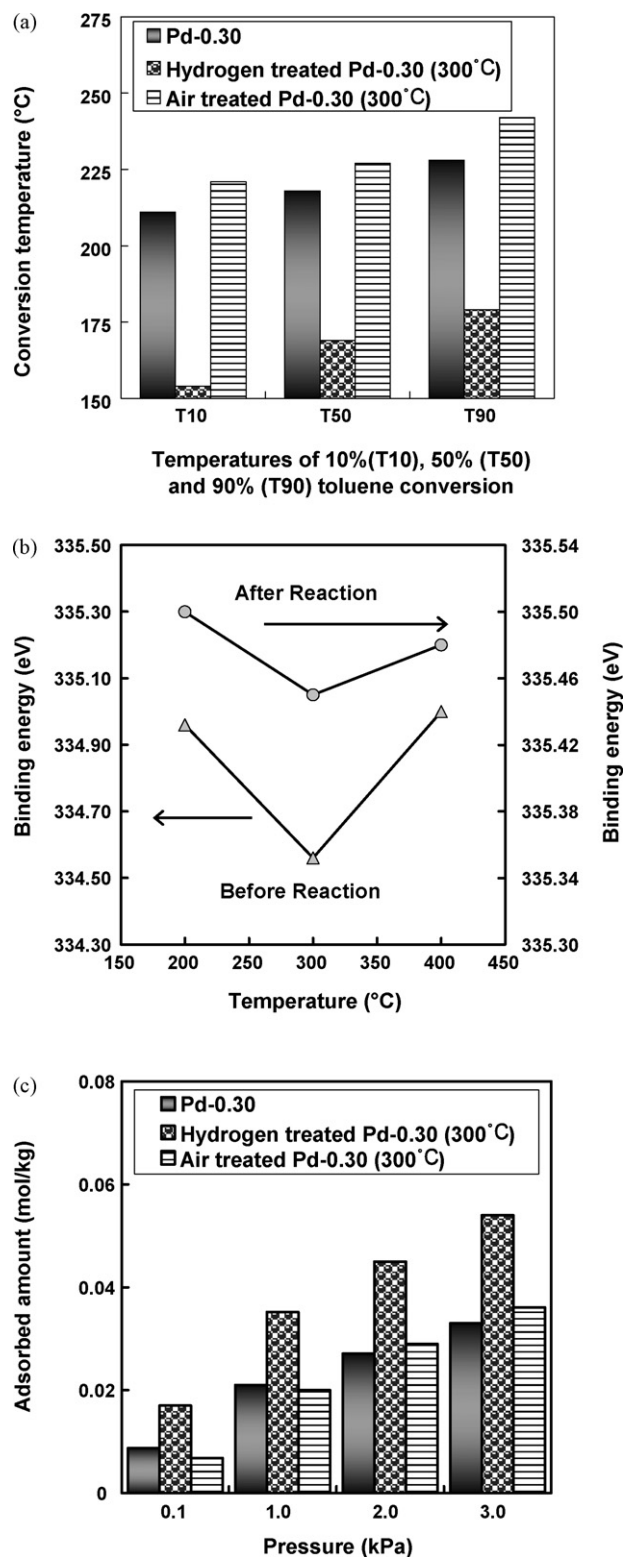| Name	BET surface area (m² g⁻¹)	Metal surface area (m² g⁻¹)	T_{10} (°C)	T_{50} (°C)	T_{90} (°C)
Parent (Pd-0.30)	65.1	0.15	211	218	228
Air pretreatment					
Pd-AT (200 °C)	67.5	–	220	226	235
Pd-AT (300 °C)	68.5	–	221	227	242
Pd-AT (400 °C)	68.6	–	219	225	227
Hydrogen pretreatment					
Pd-HT (200 °C)	66.7	–	157	174	182
Pd-HT (300 °C)	67.6	–	154	169	179
Pd-HT (400 °C)	71.6	–	161	183	197

(a)

(b)

(c)

Fig. 1. Comparison plot of conversion temperatures of T_{10}, T_{50}, T_{90} on Pd-0.30, hydrogen treated Pd-0.30 (Pd-HT-300 °C) and air treated Pd-0.30 (Pd-AT (300 °C)) (Reaction condition: catalyst weight = 1.0 g: toluene concentration = 1000 ppm in air; GHSV = 8000 h^{-1}) (a), binding energies (BE) of the Pd 3d$_{5/2}$ for hydrogen treated Pd-0.30 (Pd-HT (300 °C)) before and after toluene oxidation (b) and comparison plot of adsorption isotherm of toluene on Pd-0.30, hydrogen treated Pd-0.30 (Pd-HT (300 °C)) and air treated Pd-0.30 (Pd-AT (300 °C)) (c).
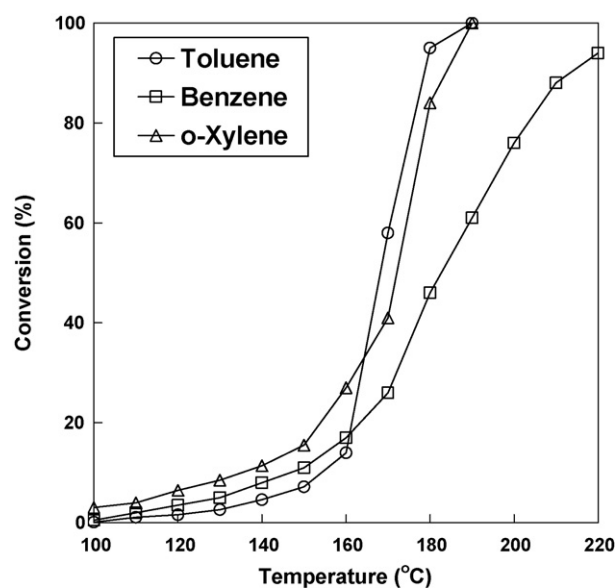

Fig. 2. Conversion profiles of BTX oxidation on the hydrogen treated Pd-0.30 (Pd-HT (300 °C)). (Reaction condition: catalyst weight = 1.0 g: BTX concentration = 1000 ppm in air; GHSV = 8000 h^{-1}).

related with the ionization potentials of methyl derivatives [15]. Fig. 2 shows the behavior of BTX conversion over the hydrogen pretreated Pd-0.3 catalyst (Pd-HT (300 °C)). The order of catalytic activities greatly changed with an increasing reaction temperature [14]. This means that the system does not follow the general pattern under T_{25} (o-xylene > benzene > toluene) although the catalytic activities for BTX oxidation above T_{25} highly coincides with the results reported in the literature (toluene > o-xylene > benzene).

3.2.2. Adsorption

The adsorption equilibrium isotherms of VOCs on the pre-reduced catalyst (Pd-HT (300 °C)) were measured in a wide range of temperatures and pressures to characterize the interactions between the adsorbate and the adsorbent. Adsorption equilibrium isotherms of benzene, toluene, and o-xylene at three different temperatures (150, 175 and 200 °C) on the hydrogen pretreated Pd catalyst are shown in Fig. 3(a–c). As shown in this figure, the adsorbed amount of o-xylene obtained on the sample catalyst at all temperatures is much lower than that of other adsorbates. However, in the case of toluene and benzene, the order of adsorption capacity was reversed with an increase in the system temperature. In other words, although the adsorption capacity of toluene is by far the larger than that of benzene at 150 °C, the difference in adsorbed amounts between the two adsorbates at 175 °C is negligible, and the adsorbed amount of toluene is slightly lower than that of benzene at 200 °C. The results obtained did not follow the general relationship between the molecular weight and the adsorption capacity. In addition, the trend of the catalytic oxidation of BTX could not be correlated with the order of the adsorption equilibrium amount of BTX.

Several types of adsorption isotherms have been widely used and tested to represent various adsorption-based systems. Recently, Echard and Leglise [30] have used mobile, localized, and multi site adsorption models to explain the adsorption characteristics of H$_2$S on a sulfided CoMo/Al$_2$O$_3$ catalyst. Among the tested models, two sites (L2) localized adsorption models having two different types of adsorption sites, namely, the metal phases and the catalytic support, represented the best result.
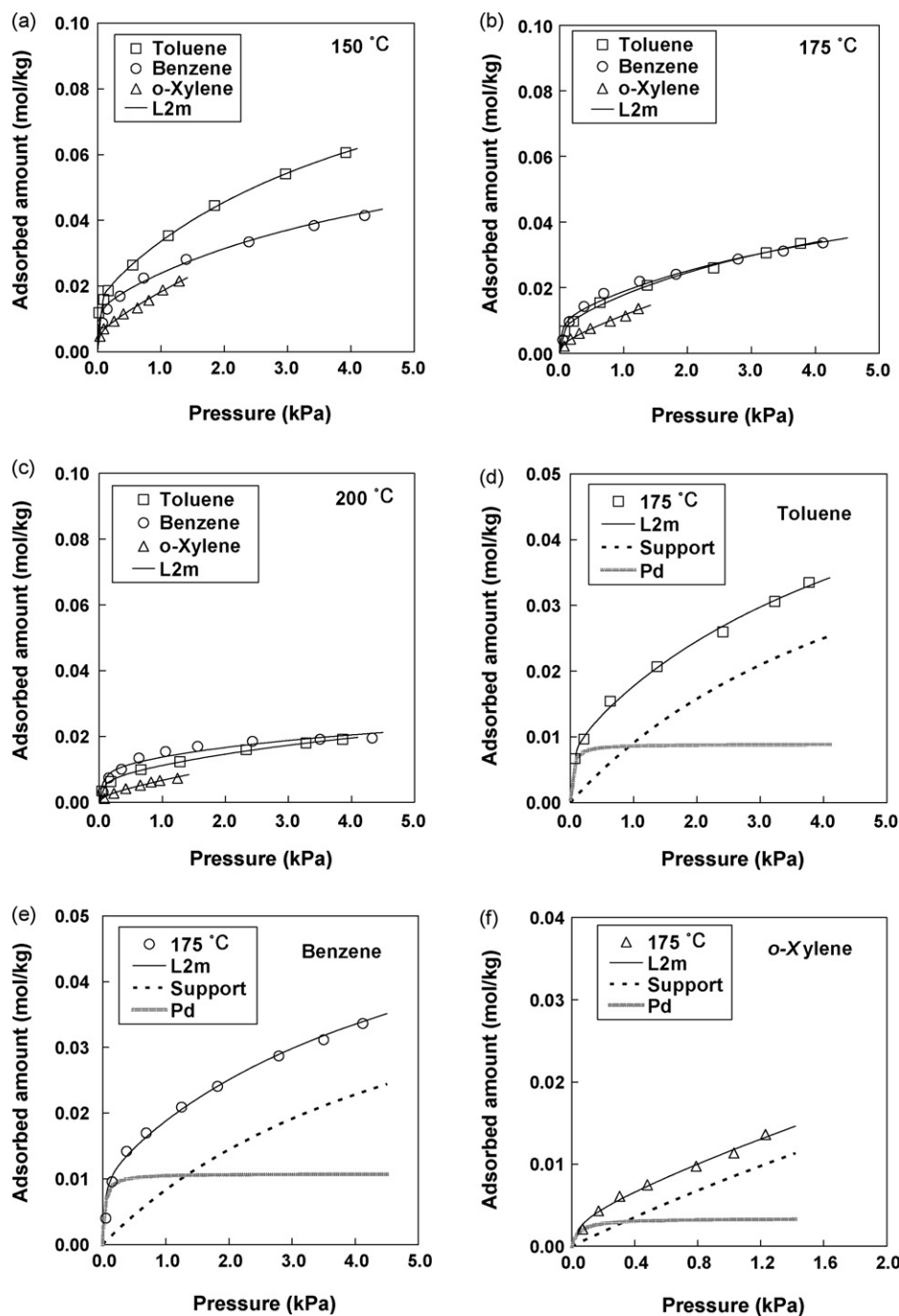
Fig. 3. Adsorption isotherms of BTX on the hydrogen treated Pd-30 (Pd-HT (300 °C)) at 150 °C (a), 175 °C (b) and 200 °C (c) and validation of the L2m isotherm model for the toluene (d), benzene (e) and o-xylene (f) on the hydrogen treated Pd-0.30 (Pd-HT (300 °C)).

Although the metal supported catalyst has many kinds of adsorption sites, the proposed equation was reliable and suitable for treating the supported catalyst. The two sites localized Langmuir equation (L2m) is as follows:

$$N = m \left[\frac{(1-f)K_a\,p}{1+K_a\,p} + \frac{f K_m\,p}{1+K_m\,p} \right] \tag{1}$$

where p is the equilibrium pressure, N is the adsorbed moles, m is the maximum adsorbed amount, f is the fraction of the adsorbed amount, and K_a and K_m are Henry's law adsorption constants for the catalytic support and the metal phase, respectively. The parameters such as m, K_a and K_m are temperature dependent. A

pattern search algorithm called Nelder–Mead simplex method was used to determine the adsorption isotherm parameters from the experimental data [31]. The objective function used is based on the square of residuals (SOR), which is an absolute value and the magnitude of the value determined is also closely related with its accuracy and the number of experimental points [32]. The SOR was expressed as follows:

$$SOR = \frac{1}{2} \sum (N_{exp} - N_{cal})^2 \tag{2}$$

where N_{cal} and N_{exp} are the calculated and experimental amounts adsorbed, respectively.

Table 3
Adsorption isotherm parameters of benzene, toluene and o-xylene on hydrogen (300 °C) pretreated Pd-0.30 catalyst (Pd-HT (300 °C))

Temperature (°C)	m (mol kg^{-1})	f (−)	K_a (kPa^{-1})	K_m (kPa^{-1})	SOR
Benzene					
150	0.079	0.178	0.1829	56.426	1.525×10^{-5}
175	0.065	0.166	0.1813	32.152	8.342×10^{-6}
200	0.035	0.304	0.1683	18.367	9.479×10^{-6}
Toluene					
150	0.115	0.150	0.206	61.587	2.705×10^{-6}
175	0.069	0.129	0.179	31.143	1.053×10^{-6}
200	0.044	0.175	0.126	15.789	1.624×10^{-7}
o-Xylene					
150	0.118	0.055	0.120	47.882	5.244×10^{-7}
175	0.086	0.039	0.112	21.235	4.352×10^{-7}
200	0.054	0.042	0.096	11.882	2.215×10^{-7}

As shown in Fig. 3(a–c), the L2m models (thick solid lines) were satisfactorily correlated with the adsorption data for the pressure and temperature range studied. Table 3 also presents the isotherm parameters determined by SOR values. The estimated values of m, K_a and K_m were found to decrease with increasing temperature. To examine the relative contributions of metal and support to the adsorption properties of the sample, the adsorption isotherms of BTX at 175 °C were compared as shown in Fig. 3 (d–f). The results obtained have a similar pattern. In other words, the thick grey lines representing the adsorption capacities of BTX on the Pd phase are sharply increased at lower pressures, and then they approached a horizontal plateau, whereas the adsorption amounts of BTX on alumina support (dotted line) gradually increased with pressure. The influence of the Pd phase on the adsorbed amount of BTX is comparatively larger than that of the support at relatively lower pressures.
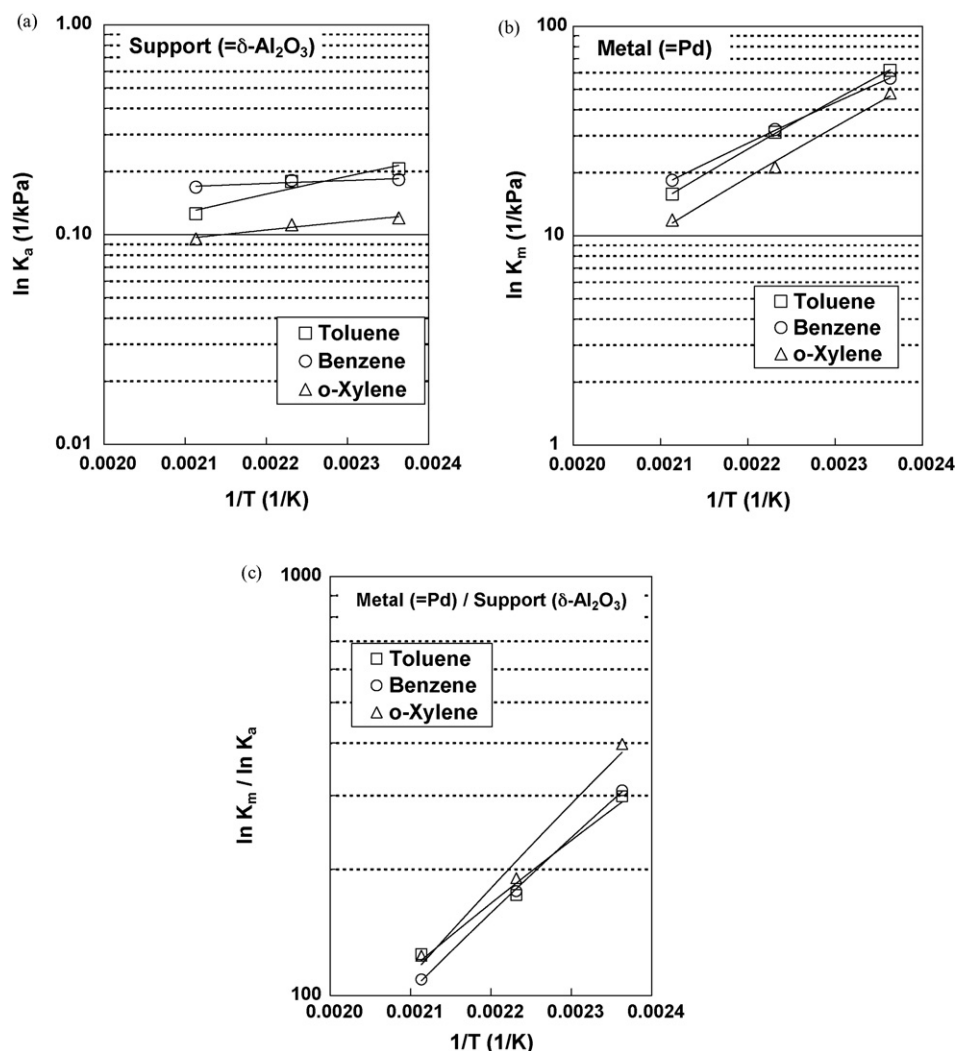

Fig. 4. Adsorption affinities of BTX on support (K_a) (a), on palladium phase (K_m) (b) and the relative ratios (K_m/K_a) of adsorption affinities (c).

3.2.3. Adsorption affinity

To assess the adsorption affinity for the selected adsorbates, Henry's constants were calculated by using the L2m isotherm equation and as plotted in Fig. 4. The estimated Henry's constant values linearly decreased with temperature. As can be noted in Table 3, the estimated parameters of the Pd phase (K_m) were also much larger than that of the alumina support (K_a) for BTX adsorbates. With the L2m isotherm equation, the K_m values were determined to be 109–308 times for benzene, 126–299 times for toluene, 124–398 times for o-xylene than K_a, indicating that the Pd phase plays a key role in controlling the adsorption system.

On the other hand, the sequence of Henry's constant is quite different. Although Henry's constant values for o-xylene are lower than that of toluene and benzene (Fig. 4a and b), the relative ratio (K_m/K_a) of Henry's constant for o-xylene is larger than that of toluene and benzene (Fig. 4c). In addition, the magnitudes of adsorption affinities for the metal phase and the support at high temperature (200 °C) were in the order of benzene > toluene > o-xylene, which conforms to the increasing the molecular weights (or decreasing ionization potentials). However, the order of adsorption affinities for BTX was not identical with the order of the molecular weight (or the ionization potentials) as the temperature decreased. It was also observed that Henry's constants for benzene and toluene were more dependent on the temperature than those of o-xylene. In other words, the order of adsorption affinity between benzene and toluene was reversed when the temperature was above (or below) 175 °C. In addition,

considering the relative ratios of Henry's constant, the pre-reduced catalyst (Pd-HT (300 °C)) has more affinity to o-xylene exhibiting the lowest values for the metal and the support than its affinity to other adsorbates. On the whole, the result is in good agreement with the pattern of catalytic oxidation of BTX as described above. The order of the relative ratio of Henry's constant is well correlated with the order of catalytic activity for BTX.

3.2.4. Isosteric heat of adsorption

The isosteric heats of adsorption (q_{st}) were obtained from the adsorption isotherm data using the Clausius–Clapeyron equation to understand the interaction properties of the catalyst.

$$\frac{q_{st}}{RT^2} = \left[\frac{\partial \ln p}{\partial T}\right]_N \tag{3}$$

where p is the pressure, T is the temperature, N is the adsorbed moles, and R is the gas constant. The variation of isosteric heat of adsorption is closely related to the combined interaction of the adsorbent–adsorbate molecules and the adsorbate–adsorbate in the adsorbed phase. The trend of isosteric heat curve is constant and independent of the coverage when the system follows the ideal Langmuir case having the energetic equivalence for all adsorption sites. On the other hand, in the case of an energetically heterogeneous and non-uniform surface, the behavior of isosteric heat of adsorption varies with the surface coverage. The isosteric heats of adsorption as a function of the adsorbed amount for three different molecules (benzene, toluene, and o-xylene) on the
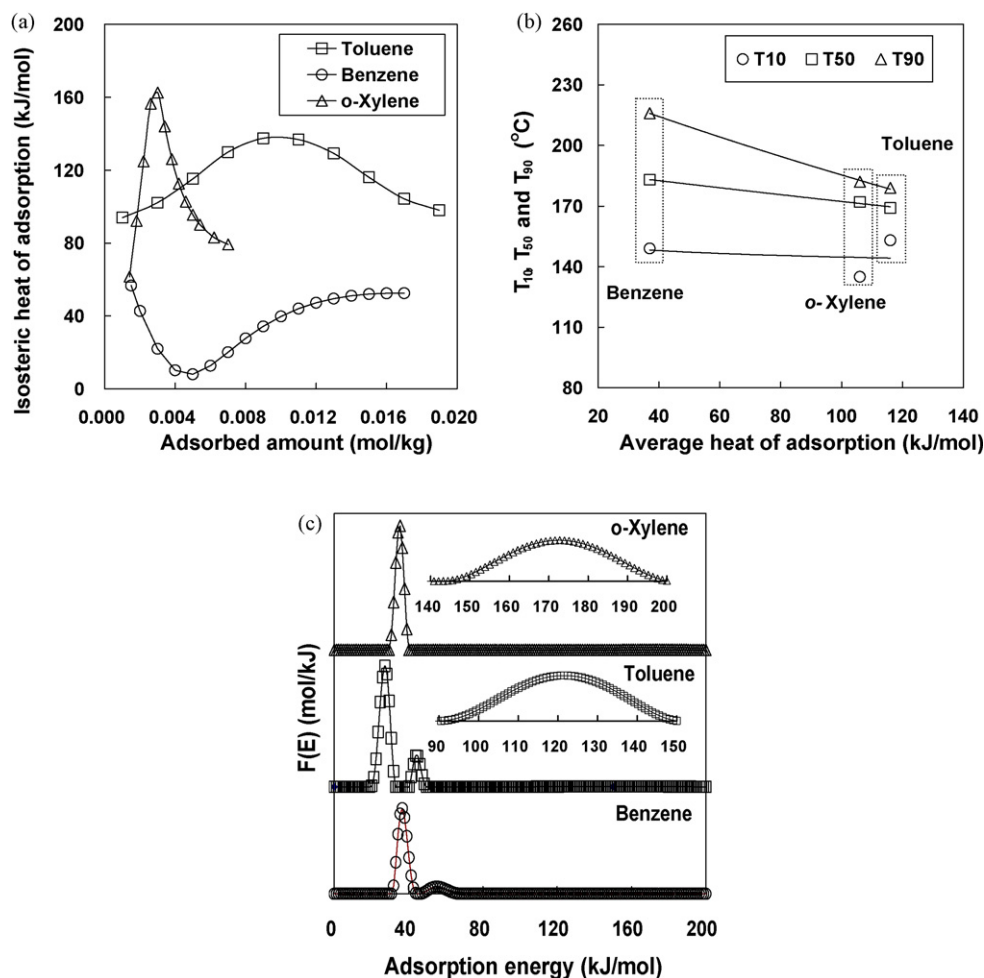

Fig. 5. Isosteric heat of adsorption of BTX (a), influence of average isosteric heat of adsorption on T_{10}, T_{50} and T_{90} for BTX (b) and adsorption energy distributions of BTX (c).

hydrogen pretreated sample (Pd-HT (300 °C)) are shown in Fig. 5(a). As shown in this figure, the heat curves can be classified into two groups. A similar degree of adsorption energy sites has been noticed in the adsorption of toluene and o-xylene. Namely, the heat curves for toluene and o-xylene significantly rose to a maximum (0.003 mol kg^{-1} for o-xylene and 0.009 mol kg^{-1} for toluene) and then continuously decreased as the loading increased. In addition, the isosteric heat values of toluene and o-xylene were also greatly higher than that of benzene. This corresponds to the region of the chemisorption. On the other hand, the isosteric heat curve for benzene severely decreased toward the minimum (0.005 mol kg^{-1}) and then monotonically increased as the adsorbed amount increased. In other words, the benzene–adsorbent (or catalyst) interaction dominated the system in the initial region and as the adsorbed amount increased, the lateral (adsorbate–adsorbate) interactions controlled the system. The general order of the magnitudes of average isosteric heat of adsorption was toluene (116 kJ mol^{-1}) > o-xylene (106 kJ mol^{-1}) > benzene (37 kJ mol^{-1}). This result clearly shows that aromatics involving methyl derivatives have relatively higher isosteric heat values compared to that of benzene. Previous studies have reported that benzene is less reactive than aromatic molecules having methyl derivatives and lower ionization potentials in the catalytic oxidation of VOCs [15].

Fig. 5(b) shows the influence of isosteric heat of adsorption on T_{10}, T_{50} and T_{90} for BTX conversion over the hydrogen pretreated sample (Pd-HT (300 °C)). This result also supports that the catalytic activities depend on the isosteric heat of adsorption. The reaction temperatures for BTX gradually decrease with increasing average heat of adsorption. For example, temperatures for 90% BTX conversion were 216 (benzene), 182 (o-xylene) and 179 (toluene) °C, respectively. In addition, the higher the isosteric heat of adsorption, the smaller the degree of difference between T_{10}, T_{50} and T_{90}. Thus, the magnitude of the isosteric heat of adsorption of BTX would be the main factor of the catalytic activity.

3.2.5. Adsorption energy distribution

To get information on the surface energy heterogeneity of a porous media, we used the distribution function and the local adsorption isotherm as well as the experimental adsorption equilibrium data [33,34]. The overall adsorption isotherm on the heterogeneous solid surface can be written in the form of

$$\theta(p) = \int_{E_{\min}}^{E_{\max}} \theta(p, E) \cdot F(E) \cdot dE \tag{4}$$

where p is the equilibrium pressure, E is the adsorption energy, $F(E)$ is the adsorption energy distribution function, $\theta(p, E)$ is a local adsorption isotherm with an adsorption energy, and $\theta(p)$ is the experimental adsorption isotherm data. The Fowler Guggenheim isotherm equation was used as a kernel function for this system to describe the localized monolayer adsorption with lateral interaction. The Fowler Guggenheim (FG) equation can be expressed as follows:

$$\theta(p, E) = \frac{K \cdot p \cdot \exp(zw\theta/k_B T)}{1 + K \cdot p \cdot \exp(zw\theta/k_B T)} \tag{5}$$

where T is the absolute temperature, p is the equilibrium pressure, z is the number of closest adjacent molecules in the monolayer, w is the interaction energy between the two nearest neighboring molecules, k_B is the boltzmann constant, $K = K_0(T) \exp(E/k_B T)$ is the Langmuir constant, and $K_0(T)$ is the pre-exponential factor which can be obtained from the partition functions for an isolated molecule. The corresponding values $(K_0(T))$ for BTX were calculated based on the literature [33,34]. To get stable solutions,

the generalized nonlinear regularization method was adopted with the regularization parameter $\alpha = 1 \times 10^{-3}$ [35–38].

Fig. 5(c) shows the calculated adsorption energy distributions for toluene, benzene and o-xylene on the hydrogen treated Pd-based sample (Pd-HT (300 °C)). Interestingly, the adsorption energy distribution curves for toluene molecules have three peaks, while the curves for benzene and o-xylene reveal two peaks. Previous studies have shown that the number of peaks of adsorption energy distribution was closely related with the sample molecules which indicate the structural differences [33,34]. Clear differences were noticed in the calculated values of the adsorption energy distribution functions for BTX. In other words, the distribution curves for toluene show two pronounced peaks that appeared at 27.5 and 45.3 kJ mol^{-1} with a tiny peak at 121.6 kJ mol^{-1}. In addition, the energy intensity of the first peak is nearly 4 times larger than that of the second. In the case of benzene, the main peak appears at 36.4 kJ mol^{-1} with minor peak appearing at 55.0 kJ mol^{-1}. The maximum of the adsorption energy distribution for o-xylene was 35.5 kJ mol^{-1}, and the lower energy peak was also between 94.1 and 150.0 kJ mol^{-1} with a tiny peak at 172.8 kJ mol^{-1}. Interestingly, the relatively high adsorption energy peaks were observed for the lower ionization potentials (or the higher Debye dipole moments). The results led us to conclude that two (benzene and o-xylene) or three (toluene) different kinds of surface energetic heterogeneities exist on the hydrogen treated catalyst. It was also observed that these adsorption energy curves were in the similar ranges that were determined from the isosteric heat of adsorption. Therefore, these results strongly support that the overall catalytic oxidation of BTX largely depends on the surface characteristics of the catalyst rather than on the adsorbed amount of BTX.

4. Conclusions

In this work, the influence of catalyst pretreatments on the adsorption and catalytic activities of BTX over the supported Pd and its pretreated catalysts was studied. The catalytic behaviors and adsorption properties of BTX were found to be highly dependent on the pretreatment conditions. The oxidation state and the surface energy characteristics of Pd on the support play a major role in the adsorption and catalytic system. Pre-reduced Pd/Al$_2$O$_3$ catalysts presented a higher catalytic activity and adsorption capacity for BTX oxidation and adsorption. In addition, the feature of catalytic oxidation of BTX was found to vary with a reaction temperature. The two sites localized Langmuir equation (L2m) isotherm model provided useful information and good correlation of adsorption of BTX. The result of adsorption affinity for BTX indicated that the supported metallic phases have a much stronger adsorption affinity than that of the alumina. Moreover, the order of the relative ratio of adsorption affinity is in good agreement with the patterns of the catalytic oxidation of BTX. The isosteric heats of adsorption for methyl derivatives of benzene are significantly higher than benzene. The higher isosteric heat of adsorption requires lower reaction temperatures for BTX conversion. In addition, a comparative analysis of the adsorption energies indicates that the parent and its modified catalysts have different types of surface energetic heterogeneities.

Acknowledgement

References

[1] E.N. Ruddy, L.A. Carroll, Chem. Eng. Prog. 89 (1993) 28–35.

[2] I. Khan, A.K. Ghoshal, J. Loss. Prevent. Proc. 13 (2000) 527–545.
[3] K. Everaert, J. Baeyens, J. Hazard. Mater. B: Environ. 109 (2004) 113–139.
[4] M. Guillemot, J. Mijoin, S. Mignard, P. Magnoux, Appl. Catal. B: Environ. 75 (2007) 249–255.
[5] E.M. Cordi, J.L. Falconer, J. Catal. 162 (1996) 104–117.
[6] B. Grbic, N. Radic, A. Terlecki-Baricevic, Appl. Catal. B: Environ. 50 (2004) 161–166.
[7] T. Garcia, B. Solsona, D.M. Murphy, K.L. Antcliff, S.H. Taylor, J. Catal. 229 (2005) 1–11.
[8] J. Tsou, P. Magnoux, M. Guisnet, J.J.M. Órfão, J.L. Figueiredo, Appl. Catal. B: Environ. 57 (2005) 117–123.
[9] R.S.G. Ferreira, P.G.P. de Oliveira, F.B. Noronha, Appl. Catal. B: Environ. 50 (2004) 243–249.
[10] T. Garcia, B. Solsona, D. Cazorla-Amoros, A. Linares-Solano, S.H. Taylor, Appl. Catal. B: Environ. 62 (2006) 66–76.
[11] A.F. Pérez-Cadenas, S. Morales-Torres, F. Kapteijn, F.J. Maldonado-Hódar, F. Carrasco-Marín, C. Moreno-Castilla, J.A. Moulijn, Appl. Catal. B: Environ. 77 (2008) 272–277.
[12] S.K. Ihm, Y.D. Jun, D.C. Kim, K.E. Jeong, Catal. Today 93–95 (2004) 149–154.
[13] P. Dege, L. Pinard, P. Magnoux, M. Guisnet, Appl. Catal. B: Environ. 27 (2000) 17–26.
[14] S.C. Kim, S.W. Nahm, W.G. Shim, J.W. Lee, H. Moon, J. Hazard. Mater. 141 (2007) 305–314.
[15] L. Becker, H. Forster, Appl. Catal. B: Environ. 17 (1998) 43–49.
[16] E. Diaz, S. Ordonez, A. Vega, J. Coca, Micropor. Mesopor. Mater. 70 (2004) 109–118.
[17] H.L. Tidahy, S. Siffert, J.F. Lamonier, R. Cousin, E.A. Zhilinskaya, A. Aboukais, B.L. Su, X. Canet, G.D. Weireld, J.M. Giraudon, G. Leclercq, Appl. Catal. A: Gen. 310 (2006) 61–69.

[18] E. Diaz, B. de Rivas, R.L. Fonseca, S. Ordonez, J.I.G. Ortiz, J. Chromatogr. A 1116 (2006) 230–239.
[19] H.L. Tidahy, S. Siffert, J.F. Lamoniera, R. Cousina, E.A. Zhilinskayaa, A. Aboukaïsa, B.-L. Sub, X. Canetc, G. De Weireldc, M. Frèrec, J.-M. Giraudond, G. Leclercqd, Appl. Catal. B: Environ. 70 (2007) 377–383.
[20] A. O'Malley, B.K. Hodnett, Catal. Today 54 (1999) 31–38.
[21] H. Huang, Y. Liu, W. Tang, Y. Chen, Catal. Commun. 9 (2008) 55–59.
[22] J.C.S. Wu, Z.A. Lin, F.M. Tsai, J.W. Pan, Catal. Today 63 (2000) 419–426.
[23] A.A. Barresi, G. Baldi, Ind. Eng. Chem. Res. 33 (1994) 2964–2974.
[24] C.H. Wang, S.S. Lin, Appl. Catal. A: Gen. 268 (2004) 227–233.
[25] S.C. Kim, J. Hazard. Mater. B91 (2002) 285–299.
[26] W.G. Shim, J.W. Lee, H. Moon, J. Chem. Eng. Data 48 (2003) 286–290.
[27] J.W. Lee, W.G. Shim, H. Moon, Micropor. Mesopor. Mater. 73 (2004) 109–119.
[28] D. Lomot, W. Juszczyk, Z. Karpinski, Appl. Catal. A: Gen. 155 (1997) 99–113.
[29] M. Skotak, D. Lomot, Z. Karpinski, Appl. Catal. A: Gen. 229 (2002) 103–115.
[30] M. Echard, J. Leglise, Therm. Acta. 379 (2001) 241–254.
[31] J.B. Riggs, An Introduction to Numerical Methods for Chemical Engineers, Texas Tech. University Press, Lubbock, 1988.
[32] A. Malek, S. Farooq, AIChE J. 42 (1996) 3191–3201.
[33] M. Jaroniec, R. Madey, Physical Adsorption on Heterogeneous Solids, Elsevier, Amsterdam, 1988.
[34] W. Rudzinski, D. Everett, Adsorption of Gases on Heterogeneous Solid Surfaces, Academic Press, London, 1991.
[35] T. Roth, M. Marth, J. Weese, J. Honerkamp, Comput. Phys. Commun. 139 (2001) 279–296.
[36] M.V. Szombathely, P. Brauer, M. Jaroniec, J. Comput. Chem. 13 (1992) 17–32.
[37] A.M. Puziy, T. Matynia, B. Gawdzik, O.I. Poddubnaya, Langmuir 15 (1999) 6016–6025.
[38] W.G. Shim, J.W. Lee, H. Moon, Sep. Sci. Technol. 41 (2006) 3693–3719.